PAPER ID: 2038
DOI: 10.18462/iir.TPTPR.2021.2038

Ice thermal energy storage for electricity peak shaving in a commercial refrigeration/HVAC unit

Paola D'AGARO, Michele LIBRALATO, Gabriele TOFFOLETTI, Giovanni CORTELLA

DPIA, Università degli Studi di Udine
Udine, 33100, Italy, paola.dagaro@uniud.it

ABSTRACT

An ice thermal energy storage is adopted in the HVAC plant of a supermarket, to shave peaks in electricity use. Ice is formed at night-time by employing the commercial refrigeration system, which is considerably part-loaded during the shop closing time. During daytime, the thermal storage is discharged and operated in parallel to a water chiller, to produce chilled water for air conditioning purposes. The whole system is modelled, to look for the most effective control rule in an attempt to match energy efficiency and the need to comply with a threshold in the electricity use.

Keywords: Refrigeration, Thermal energy storage, Air conditioning, DSM

1. INTRODUCTION

Air conditioning systems in commercial buildings require a huge amount of electrical energy, ranging from minimum or even null demand at night-time to a marked maximum during the day, where the peak in the cooling load mostly corresponds to the lowest performance of the chiller due to the highest outdoor temperature. For this reason, Thermal Energy Storage (TES) is sometimes suggested to shift loads and allow a better average performance all over the day, and this is for example effectively achieved by using passive PCM slabs along the air ducts (Mosaffa and Farshi, 2016). Nonetheless, the electrical energy demand can be better managed by using TES in those cases where both time-of-use tariffs or peak tariffs are in force, in a view of Demand Side Management of the electrical grid. Cold water storage can be effectively used in this case, in order to allow the refrigerating system to accumulate cooling energy during night-time or low tariff periods and reduce electrical power demand when its cost is higher. This solution is also beneficial in terms of reducing the number of on-off cycles of the unit, thanks to the dumping effect of the water storage placed on supply line to the air handling unit (Meng et al., 2021).

Ice Thermal Energy Storage (ITES) systems are also used to increase the volumetric storage capacity and allow a greater ability to shift energy peaks. Despite the need to perform cooling at below zero temperature, which seems ineffective when compared to the typical evaporating temperature for air conditioning purposes, such systems have been investigated from both energy and exergy points of view, and encountered some interest (Sanaye and Shirazi, 2013). However, their performance and energy effectiveness are strictly correlated to their control rules, (Beghi et al., 2014) which involve a clear definition of the aim of the system. For the purpose of ITES, the cooling unit has to be operated at low evaporating temperature during the charging phase, and the cooling system has to be uncoupled from the water loop of the air handling unit, where water circulates typically at 7 °C supply temperature and 12 °C return temperature. Various configurations can be identified, depending upon the purpose of storage. If the storage is aimed at shifting the whole AC demand at night-time, the refrigerating unit operates only during the recharging phase and the AC demand is faced by discharging the storage. In contrast, if the storage is aimed just to shave peaks, a water chiller can operate in parallel to the storage during its discharge phase, to supply chilled water for the AC. In this case, the availability in the plant of separate water chiller and low temperature refrigerating unit is a plus.

In this paper the authors describe the system installed in a supermarket, where a certain synergy between the CO_2 refrigerating unit for display cabinets and cold rooms and the HVAC plant is implemented. In summertime, an ITES is implemented to store cooling energy from the refrigerating unit at night-time and make it available for AC purposes at daytime. This paper is focused on the model of the charge and discharge phases of the ITES, included in a comprehensive model of the entire system to investigate its control rules.

2. THE SYSTEM

The focus of the system is the Ice Thermal Energy Storage (ITES), i.e. a 8 m^3 thermally insulated water tank with two separate submerged cooling coils, each made of 16 mm outer diameter pipes globally 235 m long. Such cooling coils are two evaporators fed by a CO_2 booster refrigerating unit, at the same evaporating temperature as the medium temperature cabinets, t_{ev} = -10 °C. To improve the heat transfer coefficient on the water side during discharge, air is insufflated at low pressure in the storage tank. (Figure 1).

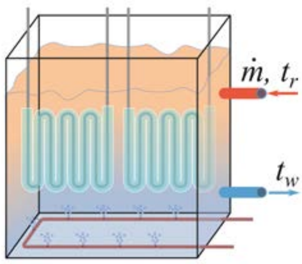

Figure 1: ITES with two evaporators in parallel, and air insufflation

On the user side, the ITES is connected through a heat exchanger to a water tank to supply the Air Handling Units (AHU). A reversible heat pump is also connected to the same water tank, in parallel to the ITES, to guarantee to meet the whole AC and heating demands (Figure 2). This configuration allows to use the Energy Storage also in wintertime, even if only with sensible heat storage, to allow some peak demand shift, reduction in on-off cycles number and heat recovery. The system is in fact also provided with further heat exchangers to recover heat from the refrigerating unit, and the thermal storage is beneficial for this purpose. However, in this paper we focus only on the summertime operation, and Figure 2 does not include heat recovery components.

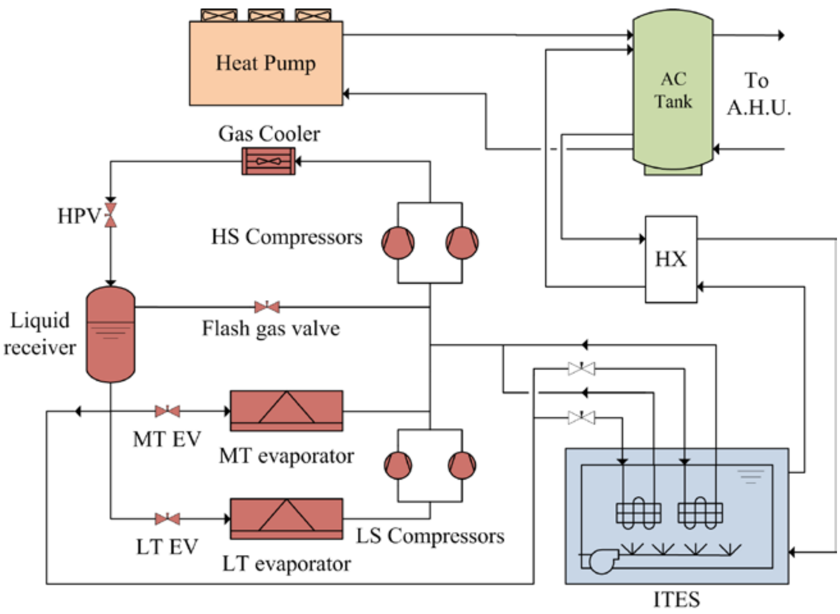

Figure 2: Sketch of the system.

The supermarket suffers a peak in the electrical energy use in the early morning, when the indoor climate conditions must be restored at the set values after the night stop, and ovens and heaters are operated to cook prepared meals for sale. On the contrary, during night-time the commercial refrigeration unit operates at part-load thanks to cabinets being closed in the absence of customers, and in favourable conditions due to the mild outdoor temperature. For this reason, an ITES was conceived to store latent energy by making ice in the tank. In the discharge phase, the storage is used until its temperature allows to cool down water in the AC circuit from 12 °C to 7 °C, which are the typical temperature values for AHU. Around 6000 kg of ice over 12 m^3 of water are expected to form, allowing for a global storage of 2250 MJ (2000 MJ latent heat, 250 MJ sensible heat up to 5 °C).

3. THE MODEL

3.1. Refrigerating unit and heat pump

The comprehensive model used to investigate the effectiveness of ITES, in terms of daily energy use or peak shifting, includes necessarily a thorough simulation of the whole system, here including the refrigerating unit and the reversible heat pump.

The commercial refrigerating unit is modelled in TRNSYS with in-house types for all components, together with the refrigerated display cabinets and the cold rooms. Through simulating the behaviour of display cabinets and cold rooms, an annual cooling capacity profile with an hourly time step can be identified, depending on some user specific configurations, like the type of cabinets (open/closed), their defrosting schedule, the opening hours of the shop, the set values for indoor temperature and humidity and so on. The cooling capacity profile we choose from previous validated simulations is faced by a CO_2 transcritical refrigerating plant, able to supply cooling at two temperature levels, for the frozen and chilled food. The model can simulate refrigerating units equipped with the most widespread solutions to improve efficiency of transcritical cycles, among which subcooling via a dedicated mechanical system (Cortella et al. 2021), parallel compression (Gullo et al., 2016) and also with heat recovery facilities to allow domestic hot water (DHW) production and space heating and cooling (D'Agaro et al., 2018, 2019) also in the view of a Demand Side Management for the electrical grid (Coccia et al., 2019). A configuration where a water storage is used for improving the efficiency of the refrigeration unit by subcooling has been also considered (Polzot et al., 2015), to investigate the feasibility of employing a high-volume fire prevention tank (950 m^3).

The reversible heat pump considered in this work is a commercial product whose performance is known from the manufacturer data as a function of the indoor and outdoor heat exchangers temperature, and load. Finally, for this application, the model in TRNSYS is linked with the code written in Matlab for the simulation of the ITES as described below.

3.2. Ice Thermal Energy Storage (ITES)

With the aim of evaluating the correct impact of the ice thermal storage on the whole system, a heat transfer analysis was made necessary.
In the specific, the two analyzed cases are the charging and the discharging modes.

3.2.1. Charge phase model

During the charging mode, the refrigeration unit, connected to the ITES on the MT line, stores cooling energy first cooling the water down to 0 °C, and then forming ice.

An analytical model developed long time ago by London and Seban (1943) was used to predict ice formation in the thermal storage. The water is assumed to be at the freezing point, and heat flow rate per unit length, flowing through the resistance composed by the ice and the internal convection, in series, is:

$$q' = \Delta t_0/(R'_{ice} + R'_0) \qquad \text{Eq. (1)}$$

Δt_0 is the temperature difference between the temperature of water at the freezing point (0°C) and the evaporating temperature, R'_{ice} is the conductive resistance of ice and R'_0 is the internal convective resistance per unit length, on the refrigerant side, assumed constant on the evaporator length and equal to its average value. In this model the external convective resistance (water side) is neglected because of the assumption on the initial temperature of water at the freezing point, and the conductive resistance of the evaporator tube is neglected.

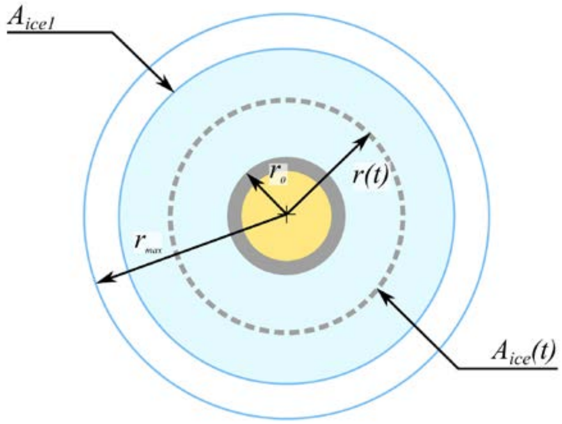

Figure 3: Schematisation of ice formation on a cylindrical surface

The heat flow rate per unit length provides the extraction of the latent heat of freezing at the surface $A_{ice}(\tau)$:

$$q' = \frac{dM_{ice}}{d\tau}\lambda_{ice} = -2\pi\rho\lambda_{ice} r \frac{dr}{d\tau} \quad \text{Eq. (2)}$$

Combining the two equations above to simplify the heat flow rate, provides the differential equation expressing radius of ice formation as a function of time:

$$2\pi\rho\lambda_{ice} r \frac{dr}{d\tau} = \frac{\Delta_t}{\left(\frac{\log\frac{r}{r_0}}{2\pi k} + \frac{1}{2\pi r_0 h_0}\right)} \quad \text{Eq. (3)}$$

where r is the radial position of growing ice and r_0 the initial radius (corresponding with the outer radius of the evaporator tube).

Since radius increases with time, the thermal resistance increases with time, and as a result the heat flow rate as well as the cooling capacity decrease.

The analytical model is able to predict the amount of ice formed as a function of the operating time of the tank. In this application, the initial water temperature is assumed to be 12°C on the basis of measured values. The estimation of the time needed to reduce water temperature down to the freezing point is based on a simple energy balance once the refrigerating power is known. In fact, measured data on the refrigerant side show that the evaporator is able to supply the full cooling capacity during this phase; furthermore, at the end of the charge phase, water is found to be at the freezing point in the whole volume. The maximum cooling capacity provided by the refrigeration unit is 70 kW.

Figure 4 gives an example of the behaviour of ITES during a charge phase, showing how the cooling capacity provided by the refrigerating unit varies during the charge time. An 8 m^3 ITES is considered, with water at 7 °C initial temperature. At the start of the process the cooling demand is limited by the refrigerating unit, since its design capacity is lower than the maximum heat flow rate which could be exchanged. Once water is chilled to the freezing point (about 1 hour) and ice builds up, its thermal resistance increases, and after a while the cooling demand decreases below the design value. If we assume to stop the charge once the outer radius of ice is 40 mm, i.e. 2.26 m^3 of ice are produced, this process takes about 5 hours, and the cooling demand at the stop of the process is reduced to 36.5 kW. It appears clearly how the thermal resistance acts in slowing down the process of ice formation and should be accounted for when estimating the charge time.

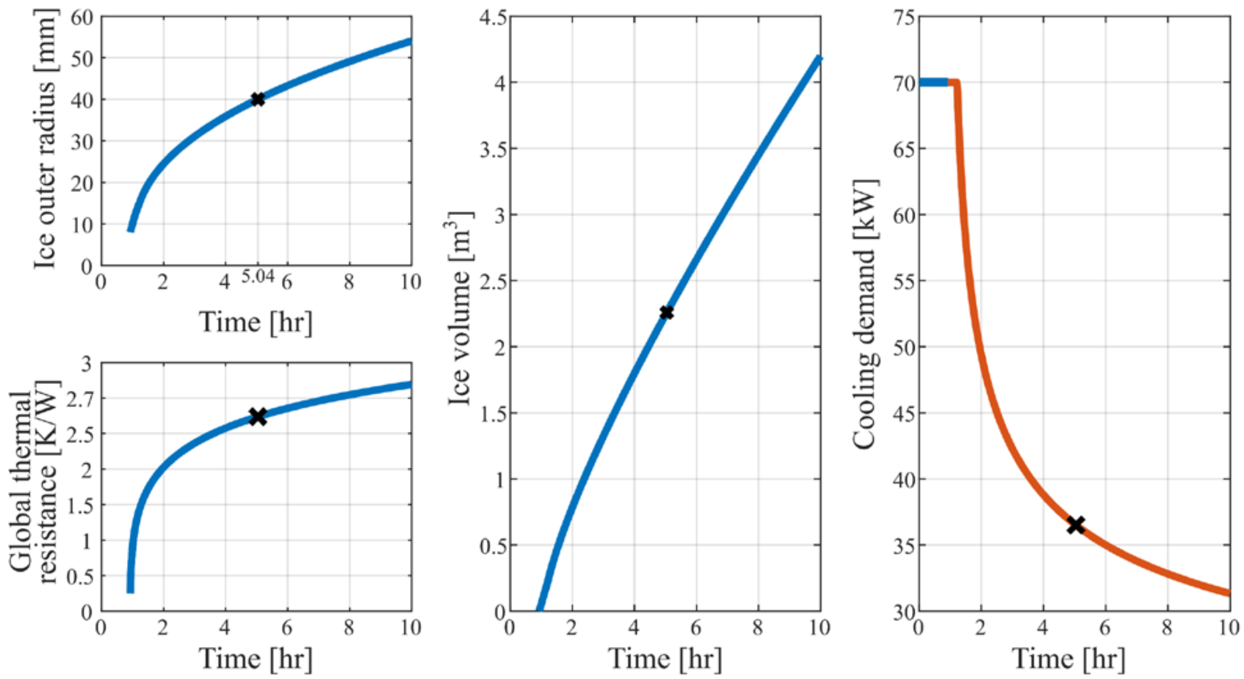

Figure 4: Ice build up and cooling demand in an example of charge phase, starting at t_w = 7°C

3.2.2. Discharge phase model

For the discharge model, an analytical solution by Lee and Jones (1996) was used to predict the ice-melt performance of the ITES. The ice cylinders were melted externally by water flowing across them. Water exiting the ITES is useful for AC purposes up to 7° C, and this parameter determines the maximum duration of the discharge phase.

A brief description of Lee's model is given below. The water temperature t_w , assumed uniform in the tank, was obtained by solving the energy balance on water mass M_{w}:

$$c_w \cdot M_w \frac{dt_w}{d\tau} = \dot{m}_{\mathrm{w}} c_w (t_{\mathrm{r}} - t_{\mathrm{w}}) + U_{env} A_{\mathrm{env}} (t_{env} - t_{\mathrm{w}}) - h_e \cdot A_{ice} \cdot (t_w - t_{ice})$$

$$- \frac{dM_w}{d\tau} \cdot c_w \cdot (t_w - t_{ice}) \qquad \text{Eq. (4)}$$

Where the left-hand side is the rate of change of internal energy, the first term at the right-hand side is the heat flux from the heat exchanger HX being $\dot{m}$ and t_r the mass flow rate of water and the return water temperature to the tank (Figure 2); the second term is the heat losses to the surrounding at temperature t_{env} ; the third term is the convective heat transfer between the water and the ice being A_{ice} the ice surface at temperature t_{ice} =0°C; the fourth term is the sensible change of the melted water which is heated from the freezing-point t_0 = t_{ice} to t_w. The mass conservation gives:

$$\frac{dM_w}{d\tau} = -\frac{dM_{ice}}{d\tau} = \frac{q_{ice}}{\lambda_{ice}} = \frac{h_e \cdot A_{ice} \cdot (t_w - t_{ice})}{\lambda_{ice}} \qquad \text{Eq. (5)}$$

Where the λ_{ice} is ice latent heat.

In Lee and Jones (1996) model the ice surface area $A_{ice}(\tau)$ is assumed to vary exponentially with time, this exponential fit has been chosen since it matches more with a physical behaviour than other trends.

$$A_{ice} = A_{ice1} exp\,(-n\tau) \qquad \text{Eq. (6)}$$

In Eq. (6), A_{ice1} is the initial ice surface area (see Figure 3), and n is obtained by the exponential curve fit between the start and the end points of the discharge period from experimental data. Once calculated the quantity of ice (from the cooling charge model) and knowing the load profile required by AC like, for example, in Figure 5, the model gives a maximum duration of the tank for the required load.

4. OPTIONS FOR USE

The plant in the configuration shown in Fig. 2 allows to pursue several goals. The main objective for the employment of ITES in the actual plant is shaving the peak in electrical energy use which occurs early in the morning in summertime, when the AC plant has to be operated since the very beginning of the day simultaneously to other high demand electric appliances. This reduction in the maximum electric power allowed a significant reduction in investment cost for the connection to the electrical grid. However, for most days in the year this problem is not likely to occur, and the ITES can be employed to implement different strategies. Through the model above described, and with the support of experimental data from the field, various strategies will be investigated in the next future. An AC cooling demand profile has been identified (Figure 5) and the feasibility of peak shaving is being explored, to reduce the chiller capacity in a view of undersizing it in future plants and taking advantage of demand tariffs. Also, specific time peak shaving strategies are going to be studied, to exploit time-of-use tariff and reduce electricity use in peak periods. In Figure 5 the possibility of supplying the whole AC demand in the early morning and to reduce chiller size are explored, starting from the quantity of ice stored at the end of the charge process shown in Fig. 4. Figure 5a represents the water temperature profiles for both the configurations, while Figure 5b shows the portion of AC cooling demand covered by the ITES. Values in blue refer to the whole AC demand supplied early in the morning by the ITES, values in ochre are for chiller size reduction. In the first case, the ITES is fully discharged after 4.7 hours, 6.8 hours in the second. In the second case, it is possible to size the chiller for a 40 kW design capacity, since the extra load is made available by the ITES.

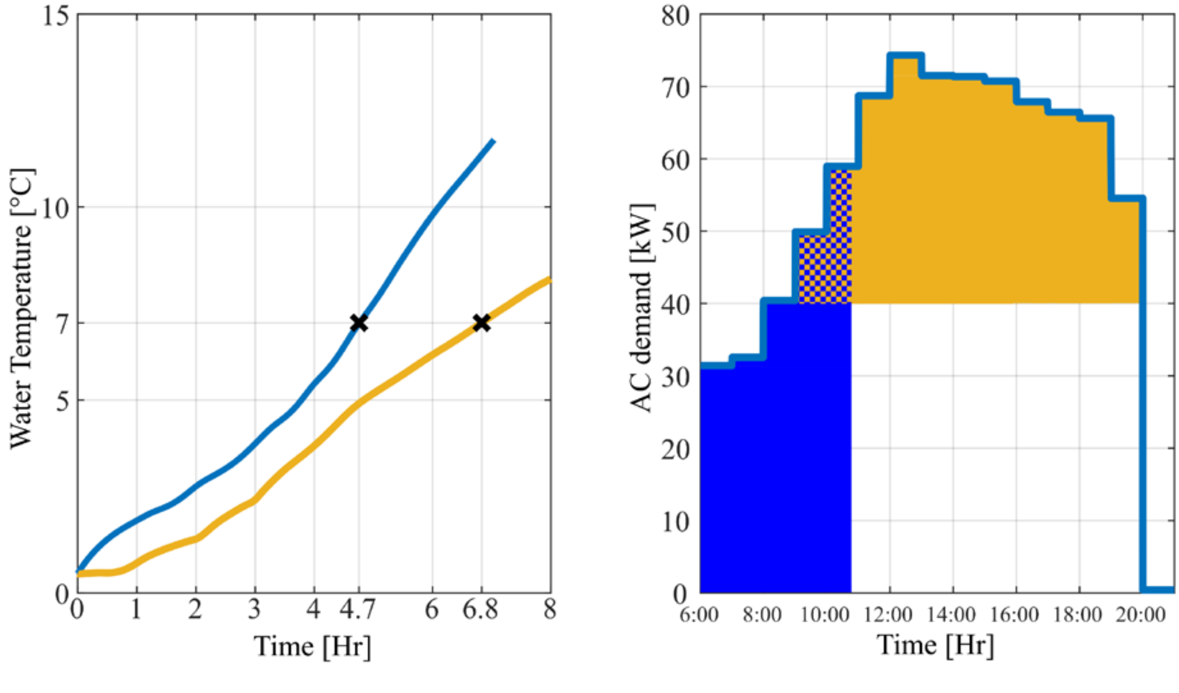

(a) (b)

Figure 5: Different ITES control strategy

Modelling shows then to be an essential tool to define the strategy of use for ITES, which can be effective tools for the Demand Side Management of electric grids. The requirement of lower evaporating pressure than chillers in order to generate ice, and heat infiltration occurring at ITES are drawbacks which are being investigated. A supermarket plant with the configuration of Figure 2 is being duly instrumented and work is in progress to validate the model and test various control strategies.

ACKNOWLEDGEMENTS

The research leading to these results has also received funding from the MIUR of Italy within the framework of the PRIN2017 project «The energy flexibility of enhanced heat pumps for the next generation of sustainable buildings (FLEXHEAT)», grant 2017KAAECT.

NOMENCLATURE

A_{ice}	Ice surface area (m^2)	r_0	Initial radial position (m)
A_{ice1}	Initial ice surface area (discharge) (m^2)	t_0	Freezing-point of water (°C)
c_w	Specific heat of water (J kg^{-1} K^{-1})	t_{ev}	Evaporating temperature (°C)
h_0	Internal convection coefficient (Wm^{-2}K^{-1})	t_{env}	Outdoor temperature (°C)
h_e	External convection coefficient (Wm^{-2}K^{-1})	t_{ice}	Ice surface temperature (°C)
k	Thermal conductivity of ice (Wm^{-1} K^{-1})	t_r	Return water temperature (°C)
$\dot{m}$	Mass flow rate of water (kg s^{-1})	t_w	Tank water temperature (°C)
M_{ice}	Mass of ice in the tank (kg)	$U_{env}A_{env}$	Overall conductance between ice tank and surroundings (Wm^{-2})
M_w	Mass of water in the tank (kg)	Δt_0	Temperature difference (t_0-t_{ev}) (K)
n	Exponential coefficient of ice melting (s^{-1})	λ_{ice}	Latent heat of fusion of ice (J kg^{-1})
R'	Thermal resistance per unit length (Wm^{-1} K^{-1})	ρ	Ice density (kg m^{-3})
r	Radial position of growing ice surface (m)	τ	Time (s)

REFERENCES

Beghi A, Cecchinato L., Rampazzo M., Simmini F., 2014. Energy efficient control of HVAC systems with ice cold thermal energy storage. Journal of Process Control, 24, 773–781.

G. Coccia, A. Arteconi, F. Polonara, G. Cortella, P. D'Agaro, 2019. Demand side management analysis of a supermarket integrated HVAC, refrigeration and water loop heat pump system. Applied Thermal Engineering, Vol. 152, 543-55.

Cortella G., Coppola M.A., D'Agaro P., 2021. Sizing and control rules of dedicated mechanical subcooler in transcritical CO_2 booster systems for commercial refrigeration. Applied Thermal Engineering, Vol. 193, paper 116953.

D'Agaro P., Coppola M.A., Cortella G., 2019. Field tests, model validation and performance of a CO_2 commercial refrigeration plant integrated with HVAC system. International Journal of Refrigeration, Vol. 100, 380-391.

D'Agaro P., Cortella G., Polzot A., 2018. R744 booster integrated system for full heating supply to supermarkets. International Journal of Refrigeration, Vol. 96, 191-200.

Gullo P., Cortella G., Minetto S., Polzot A., 2016. Overfed Evaporators and Parallel Compression in Commercial R744 Booster Refrigeration Systems– an Assessment of Energy benefits. Proc. 12th Gustav Lorentzen Natural Working Fluids Conference, 21-24 August 2016, Edinburgh, (UK), Refrigeration Science and Technology, 261-268.

Lee A. H. W., Jones J. W., 1996. "Modeling of an ice-on-coil thermal energy storage system", Energy Conversion and Management, 37 (10), 1493–1507.

London A.L., Seban R.A., 1943. Rate of Ice Formation. Transactions of the A.S.M.E., October, 771-778.

Meng Q., Li Y., Ren X., Xiong C., Wang W., You J., 2021. A demand-response method to balance electric power-grids via HVAC systems using active energy-storage: Simulation and on-site experiment. Energy Reports, 7, 762–777.

Mosaffa A.H., Fardhi L.G., 2016. Exergoeconomic and environmental analyses of an air conditioning system using thermal energy storage. Applied Energy, 162, 515-526.

Polzot A., D'Agaro P., Gullo P., Cortella G., 2015. Water storage to improve the efficiency of CO_2 commercial refrigeration systems. Proc. 24th Int. Congress of Refrigeration, 16-22 Aug 2015, Yokohama (JP), Refrigeration Science and Technology, 2765-2772.

Sanaye S., Shirazi A., 2013. Four E analysis and multi-objective optimization of an ice thermal energy storage for air-conditioning applications. International Journal of Refrigeration, 36, 828-841.

Stewart R.E., 1990. Ice Formation Rate For a Thermal Storage System. ASHRAE Transactions, 1990, 96(1): 400–405

Wang B., Li X., Zhang M., Yang X., 2003. Experimental Investigation of Discharge Performance and Temperature Distribution of an External Melt Ice-on-Coil Ice Storage Tank. HVAC&R Research, 9 (3), 291-308.